Austin Tuan and Jessica Zhu

Understanding the Formation and Evolution of Stripped Dark Matter Halos

September 22, 2015

Abstract

Although dark matter makes up 26% of our universe, scientists know very little about its properties and composition. This research on stripped dark matter halos, halos which have lost mass over time, has contributed to the overall understanding of dark matter and the universe as a whole. A new algorithm was created to model the density profiles of stripped halos as the existing Navarro-Frenk-White (NFW) fit only works well for nonstripped halos. It was determined that the slopes of the density distributions of stripped halos were steeper than what the NFW fit could accommodate. Additionally, the relationship between lambda primes, prolateness and axis ratios, and concentrations with level of stripping was examined. It was discovered that lambda prime slightly decreases, prolateness decreases, and concentration increases with a higher level of stripping, or more mass lost. From these findings, future simulations can now employ more inclusive and accurate representations of all dark matter halos as they exist currently.

1. Introduction

By current estimates, the percentage of dark matter in our universe is 26%. The critical role of dark matter in explaining the structure of the universe necessitates research like ours on its properties to fully understand its origins and properties. However, because dark matter does not absorb or emit light and thus cannot be directly observed, astronomers today must rely on large-scale simulations to model the ways in which dark matter halos interact with each other in place of concrete observations (Behroozi et al. 2013).

1.1 Dark Matter Halos

A dark matter halo is a gravitationally bound mass of dark matter particles sometimes with a baryonic galaxy at its center. For this paper, we only consider halos without such galaxies as the simulation used did not contain baryons. When halos first form, they tend to be spherical, with central regions that do not expand. However, as time passes, halo shapes change due to mass accretion and changing background densities. Halos become more elongated, with one longer axis and two shorter axes (sausage-shaped) rather than with two longer axes and one shorter one (disc-shaped) (Allgood et al. 2006). During the Big Bang, clumps of dark matter that would form halos as the universe expanded first came to light (Schramm 1993). These halos have continued to expand from the time of their creation: at a faster rate when they are younger and smaller, and more slowly once they become older and larger (Correa et al. 2015). On a larger scale, groups of dark matter halos form sheets and filaments, and much like their host galaxies, individual halos also interact with each other, merging or exchanging particles as they come into contact (Ramachandra & Shandarin 2015). As this happens, some become subhalos–smaller clusters of dark matter within a larger halo–as their mass is incorporated into the main cluster of the halo. Subhalos often confound density profiles as algorithms are unable to accurately account for their mass contribution (Bullock et al. 2001, Behroozi et al. 2013).

Ever since dark matter was first postulated to exist (Zwicky 1933) to its general acceptance in the 1980s, scientists still struggle to define its properties, from its composition to its organization. The model of the universe most widely accepted today is Lambda-Cold Dark Matter (ΛCDM), a

theory that emerged in the 1990s to conciliate disparities in observed properties of the universe: one component of this theory was cold dark matter (CDM). CDM was introduced as a way to bridge the difference between the masses of large astronomical objects as they had been calculated from gravitational effects, and those from observations of visible matter (Blumenthal et al. 1984). In the last twenty years, research about this theorized matter has been greatly advanced by the advent and development of modern-day supercomputers (Klypin et al. 2014, Prada et al. 2012).

1.2 Stripped Dark Matter Halos

Over time, a dark matter halo usually increases in mass as it merges with other smaller halos. However, a dark matter halo is classified as stripped if it loses mass over the course of its lifetime. Stripped halos are a result of halo interactions, which occur more often in denser regions as halos are more likely to interact, collide, or pass through each other (Bullock et al. 2001). As a result of these interactions, halos tend to lose large portions of their particles, resulting in a lower mass. By viewing stripped halos in the Bolshoi-Planck Simulation, a large percentage of stripped halos appear extremely elongated. Additionally, in certain mass ranges, approximately 10% of halos have lost 20% or more of their mass. Specifically, our project was focused on the structure and properties of these stripped dark matter halos.

2. Methods

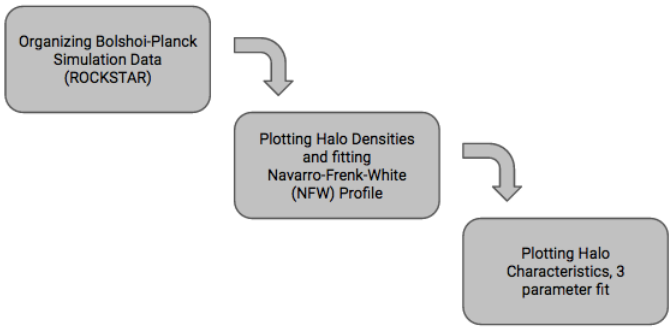

Figure 1. Procedural Flow Diagram. We followed these three main steps to obtain the results we found in our study.

All dark matter halos in this study were taken from a small portion of the Bolshoi-Planck simulation run in 2013 on NASAs Pleiades supercomputer. Each halo, dark matter particle, and relevant property–including a unique id for each halo–were given as values in a two-dimensional

array, organized by the Robust Overdensity Calculation using K-Space Topologically Adaptive Refinement (Rockstar) halo finder written by Peter Behroozi (Behroozi et al. 2013). The halos were binned by mass and level of stripping. The mass profile of each halo was then fitted to both the standard Navarro-Frenk-White profile (section 2.2.2) and a free-exponent fit. Additionally, three halo characteristics: lambda prime, prolateness, and concentration, (section 2.3) were plotted against level of stripping. The procedures mentioned above are further detailed in the following subsections.

2.1 Halo Selection and Preparation

The set of halos in our area of the Bolshoi-Planck simulation exhibited various properties in both mass and level of stripping. The mass of a halo is the combined mass of all of the particles within r_{vir}. By comparing the maximum mass, taken from the merger tree history of that halo (or its progenitor), with the current mass, we could determine the level of stripping. These halos were sorted by mass from $10^{10.2}$ to $10^{14.6} M_{\odot}$ at intervals of $10^{0.4} M_{\odot}$, and within each mass bin by percentage of mass left: 98% to 90%, 90% to 80%, 50% to 70%, 70% to 60%, and less than 60% for calculations related to the 3-parameter fit. When observing the properties of the stripped dark matter halos, the percentage of mass left was binned from 100% to 60% in 16 bins of 2.5%. A set of eight halos with minimal stripping and known to fit the Navarro-Frenk-White profile well was also created as a control. Cross-referencing the halo IDs with the particle data files, the number of particles and total mass of each halo were calculated. Position values provided in the particle tables were also used to find the distance of each particle from the center of the halo. Also given in the halo tables were the virial radius, scalar radius, lambda prime, axis ratios, and Klypin r_s. Each of these values will be used and explained in their respective subsections.

2.2 Mass Distribution Modeling

The first difference between stripped and regular dark matter halos that we explored was their mass distributions. The mass distribution of a halo is plotted as the density of dark matter particles in concentric rings radiating outward from the center of the halo. The conventional way of plotting these values are as $\log\left(\frac{r}{r_{vir}}\right)$ vs. $\log\left(density\right)$ in order to view more detail at smaller radii, as on

linear axes, the power-law decay of density provides little insight into the structure of the inner halo.

2.2.1 Virial Radius

The virial radius and scalar radius are two quantities essential to the study of halo structure. The virial radius is analogous to the radius of the halo and is calculated by finding the density of dark matter particles in the enclosed area. This radius, as defined for the Bolshoi-Planck cosmological parameters, describes the region of the halo with a density 333 times greater than the average density of the universe today, or redshift z = 0.

2.2.2 Navarro-Frenk-White Profile

The Navarro-Frenk-White (NFW) profile was a equation developed by Julian Navarro, Carlos Frenk, and Simon White (1996 &1997) to model the mass distributions of dark matter halos. In

$$\rho(r) = \frac{4\rho_s}{\frac{r}{r_s}(1+\frac{r}{r_s})^2}, \tag{1}$$

the constant ρ_s is the density at the center of the halo, and r_s is the scalar radius, which is different for each halo. According to the NFW profile, there is a specific radius within the virial radius, the aforementioned scalar radius, at which the slope of the mass distribution graph as plotted in log space would change from -1 to -3. The NFW profile is now the most commonly used equation for modeling mass distributions of halos. However, it is also recognized that while the NFW profile fits unstripped halos well, it does not do the same for stripped halos, leaving the question open and laying the foundation for our research (Navarro et al. 2004).

2.2.3 Binning

First, a simple linear binning was used for the $\log(\frac{r}{r_{vir}})$ranges. If superimposed onto the simulation, the binning would look like concentric spheres of equal difference in radii. However, because the number of particles drastically drops at larger radii, the last few bins were very sparsely populated, making the NFW profile unable to fit even the control group of halos. By using a logarithmic binning technique, the outer regions of the halo could be included without compromising the qual-

ity of the data. In the simulation, this binning would appear again as concentric spheres, but of increasing differences in radii. After implementing this change, the NFW profile became much more accurate in its modeling of the mass distributions of our eight, unstripped, control halos.

2.2.4 Accuracy Checks

As an initial check for the accuracy of our code and the fitting algorithm used to optimize the NFW profile, the calculated r_s value was compared to the r_s given in the Rockstar tables. Although small discrepancies in the values could be attributed to differences in binning methods or other minor coding preferences, any large errors would be an explicit indication of some problem with the optimization code. After the preliminary value check, the produced mass distribution graphs were compared to actual pictures of the specific dark matter halos they were modeling from the simulation. By using a visual comparison, any unusual or interesting structures that appeared on the plots could be explained, and bad halos could be excluded from further analysis.

2.2.5 Fitting Functions

A Python function that calculated the least squares fit according to the Levenberg-Marquardt algorithm was used for all instances where a curve was fitted to original data. The fit optimizes the model curve in such a way that the squares of the deviations between the data and the curve is at a local minimum. First, the Navarro-Frenk-White profile was fit to our set of stripped dark matter halos as a basis for improvement on the current model, feeding the algorithm two parameters: r_s and ρ_s. Then, the profile was slightly altered so that the second exponent could be left as a third free parameter n to be optimized using the Levenberg-Marquardt algorithm as seen in

$$\rho(r) = \frac{4\rho_s}{\frac{r}{r_s}(1+\frac{r}{r_s})^n}. \tag{2}$$

2.3 Properties of Stripped Dark Matter Halos

Stripped and regular dark matter halos differ in many of their properties, a result of lost or off-center mass that can cause abnormalities in halo structure and composition. We examine lambda primes, prolateness, and concentrations of stripped dark matter halos.

2.3.1 Lambda Prime

The angular momentum of dark matter halos is thought to be a result of tidal torques that grew from initial disturbances in our universe (Vitvitska et al. 2002). To study halo properties, lambda prime, a dimensionless value of angular momentum, is calculated as a function of some radius R and is defined as

$$\lambda'(R) = \frac{J}{\sqrt{2MVR}}, \tag{3}$$

where J is the total angular momentum of the particles within R, M is the mass of all the particles within R, and V is the circular velocity of R (Bullock et al. 2001). Typically, the virial radius is chosen as R, a method used in this paper.

2.3.2 Prolateness and Axis Ratios

Throughout this paper, we will refer to a term called prolateness, which is simply a variable that quantifies the shape of a halo. It is calculated as follows:

$$P = \sqrt{\frac{(\frac{b}{a})^2 + (\frac{c}{a})^2}{2}}, \tag{4}$$

where P is the prolateness, and a, b, and c are the axis lengths of a halo from longest to shortest.

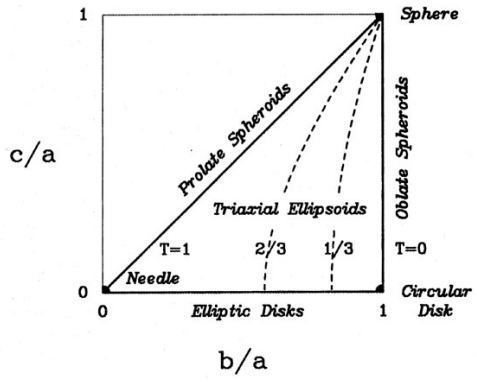

Figure 2. Elongation of Halo Based on Plots of Axes Ratios. The figure above was taken from a paper written by Zeeuw and Franx published in 1991. When the axis ratios of a halo are plotted against each other, their intersection on the graph tells what type of shape the halo follows. Halos that fall at the lower right corner of the plot tend to be more circular, as they have two longer axes and one shorter one. Halos in the upper right corner of the graph are more spherical, and they become more elongated as they move towards the lower left corner.

Figure 2 describes how a halos axes ratios relates to its shape. Such information becomes useful in determining general trends of how the shape of halos varies with its level of stripping seen later in Figure 9.

2.3.3 Concentration

Concentration has long been one of the most important and heavily studied characteristics of dark matter halos, for its intimate relationships to the composition and overall structure of such halos (Bullock et al. 2001, Prada et al. 2012). In this paper, concentration is defined as the virial radius (r_{vir}) divided by the scalar radius (r_s). Different procedures for calculating r_s may lead to different values of concentration. We will explore two methods in this paper: NFW and Klypin.

2.3.4 Scaling Factor for Concentration-Mass Relation

Since halo concentrations are known to have an existing relationship with halo mass, the concentrations were scaled based on previously calculated expressions in order to determine what effect the level of stripping alone had on the concentrations (Prada et al. 2012). For NFW concentrations,

$$\log(c) = -0.115\log(M) + 2.400, \tag{5}$$

where c is the concentration and M is the mass of the halo, was used to calculate the scaled relation and plotted against level of stripping. Eq.4 is the best fitting curve for Bolshoi-Planck centrals at z = 0, the data that we examine.

2.3.5 Kolmogorov-Smirnov Statistical Test

A two-sided Kolmogorov-Smirnov test was performed in order to determine the statistical difference between two distributions. The Kolmogorov-Smirnov statistic and its corresponding p-value were then calculated based on the null hypothesis that the two independent samples were drawn from the same distribution. A p-value less than the standard value of 0.01 signified a difference that was not negligible between the two distributions.

In our findings, some plots could easily be seen to be from different distributions simply through inspection; however, for others, in particular the graphs displaying halo axes ratios, the overlap of the numerous points on the graph creates a richness effect where one cannot easily discern the median value by eye. Consequently, a K-S test had to be conducted to be aware of certain patterns shown in the plots.

3. Results

3.1 Mass Distribution

We created mass distribution plots for 16 halos of mass between $10^{11.8}$ and $10^{12.2} M_{\odot}$ at each level of stripping and optimized both the NFW profile and our free exponent fit to them. Although plots were not created for every halo in each stripping bin, the free exponent fit was optimized for each halo, and the resulting exponent was saved into arrays at each level of stripping. Afterwards, these were graphed as histograms showing the frequency of exponents that gave the best fit for each halo at a specific stripping level.

3.1.1 Navarro-Frenk-White Profile

To test the accuracy of our code, the NFW profile was fit to eight unstripped halos. Because we were interested in only the inner regions of the halo, we fit the NFW profile up to the virial radius. Two models are shown in Figure 3.

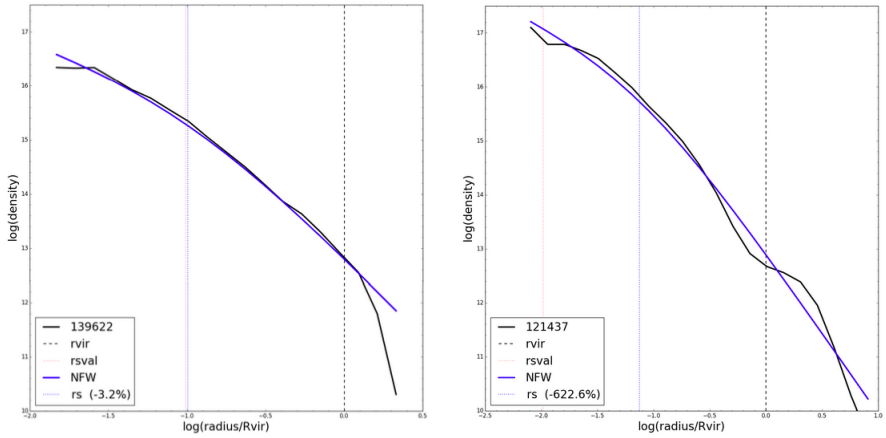

Figure 3. Mass Distributions of Halo 139622 (unstripped) and Halo 121437 (stripped). The halos mass distributions themselves are displayed in black, along with the virial radius. Superimposed in blue are the NFW profiles as optimized for these halos and the r_s values used for the fit, while the r_s as taken from Rockstar is in red.

As expected, the NFW profile fits very well up to the virial radius for the unstripped halo. The r_s value is also very similar to the one taken from the Rockstar table, with only a 3.2% deviation. However, the characteristic bump and concurrent steeper dropoff in the mass distribution of the halo 121437, seen in most of the stripped halos we plotted, is unable to be accounted for by the

NFW profile. Constricted to an outer slope of -3, the equation unsatisfactorily models the region between the r_s value and r_{vir}. In trying to compensate for this steeper slope, the optimization function also gives an r_s value that is much closer to r_{vir} than the Rockstar value, which could be attributed to differences in the optimization function code. However, it is quickly clear that, no matter where r_s is placed, the NFW profile is simply ill-equipped to model an stripped halos mass distribution.

3.1.2 Single-center vs. Multiple-center Halos

Before continuing on to the free exponent profile, we noticed that several mass distributions of the unstripped halos looked different from the others.

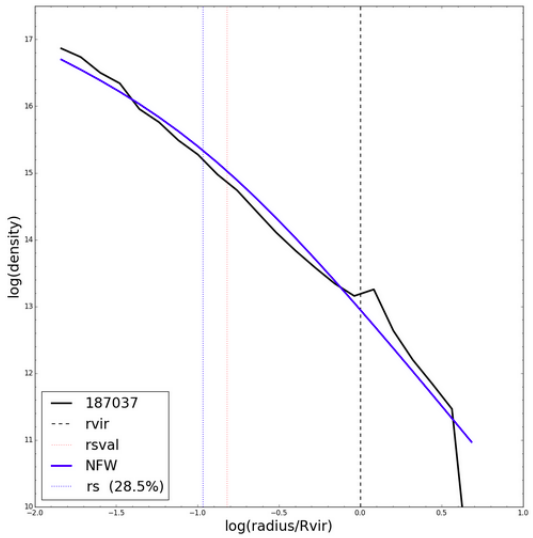

Figure 4. Mass Distribution of Halo 187037. This figure shows the mass distribution and NFW profile for the stripped halo 187037, with the same legend as Figure 3.

Instead of the smooth bump seen in many of the stripped halos such as 121437, this halos mass distribution has a sharp spike just outside of r_{vir}. The NFW profile does fit this distribution better than that of 121437; here, however, the fitted line is still never able to trace the data points as closely as in halo 187431s plot. Instead, the distribution starts above the NFW line and quickly crosses it, indicative of the datas steeper slope. In order to explain the phenomenon of this spike, we placed the mass distribution plot next to an image from the actual simulation and compared it to a picture of a stripped halo with a smoother bump alongside its mass distribution.

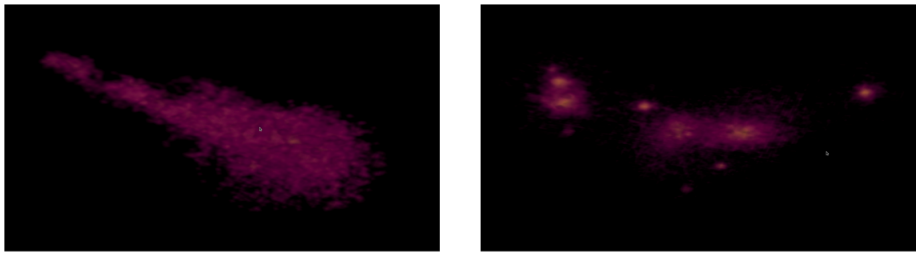

Figure 5. Snapshots of Stripped Dark Matter Halos from the Bolshoi-Planck Simulation. Above on the left and right, halos 121437 and 187037 are displayed, respectively. The mass distribution plots of the halos are seen in Figure 3.

Above are the two halos as viewed from the Bolshoi-Planck simulation. The halo on the left has a drastically elongated tail extending from its center. The halo on the right can be seen to have multiple centers, an example of stripped halos that we wish to filter out. The latter is usually a result of errors in the simulation coding and their density distributions have a characteristic bump that indicates excess substructure outside the virial radius of the central halo. To study only true stripped dark matter halos, we would need to clean our data set of any halos with multiple centers.

3.1.3 Free-Exponent Profile

Across the board, the stripped halos had mass distributions with an outer slope greater than -3. Therefore, we used the free exponent fit to gather more information about the characteristics of the halo at further radii. By allowing the exponent to be optimized to the distribution curve, the fit could account for that steeper slope and output its value. However, fitting the profiles up to r_{vir} negated any improvement of the free exponent fit from the NFW fit.

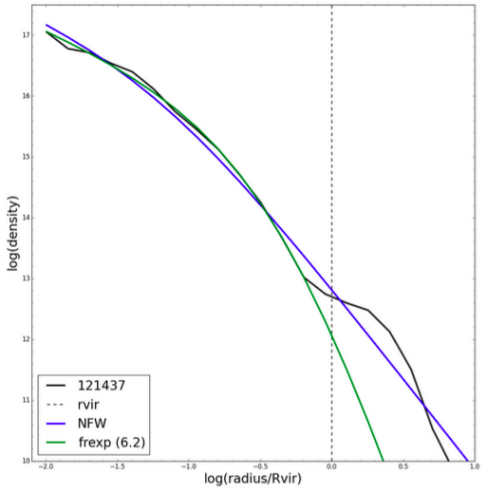

Figure 6. Mass Distribution of Halo 121437. This figure shows the free exponent fit for a stripped halo in green. Here the rsvalues are disregarded because the value of the exponent directly correlates with the rserror, and the free exponent profiles rs is always closer to rvir, suggesting that a greater outer slope simply takes longer to transition to.

In accounting for the bump, the free exponent fit would underestimate the slope outside r_s. Thus, in order to make the optimization more accurate, we created an algorithm to fit the profiles only up to the bump rather than r_{vir}.The free exponent error is clearly shown to be a better fit for the mass distribution for this halo. In this case, the second term of the denominator is to the 6.2 power, signifying an outer slope of -7. However, leaving the exponent completely unrestrained or undefined is problematic because it leaves us with no indication of what variables it is a function. The exponents vary across the different masses and levels of stripping, and even within a single bin. In order to observe general trends in the free exponent profiles of these stripped dark matter halos, we need to condense the data into a single graph that could represent every halo in our data set.

Instead of printing individual mass distribution plots for each halo in our data set, we first created histograms comparing the previously mentioned four levels of stripping in both the $10^{11.4}$ to $10^{11.8} M_\odot$ and $10^{11.8}$ to $10^{12.2} M_\odot$ mass bins. Then, the data from these 8 histograms were condensed again, producing Figure 7, which plots the median exponent from each histogram as a function of the fraction of mass remaining.

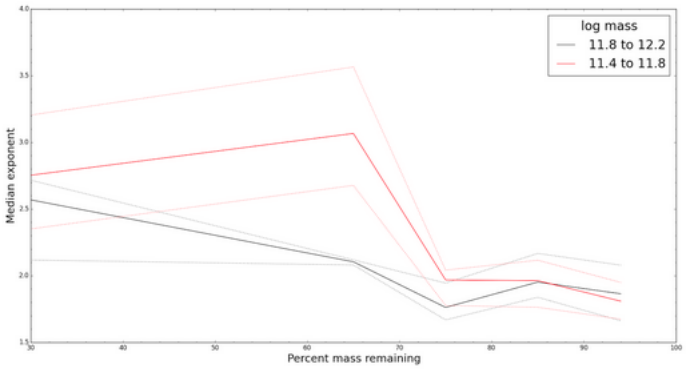

Figure 7. Histogram of exponents from the free exponent profile at two log mass ranges. The solid lines indicate the median exponent at each level of stripping, and the dotted two dotted lines mark the 40th and 60th percentiles. The noise in the plots was due to the restricted data set; the number of halos in each bin was often less than 15.

From Figure 7, it can be seen that the magnitudes of the free exponent tend to increase with a higher level of stripping, or a lower percentage of mass remaining. Additionally, a halos from the lower mass range had higher median exponents than those from the higher range.

3.2 Lambda Prime

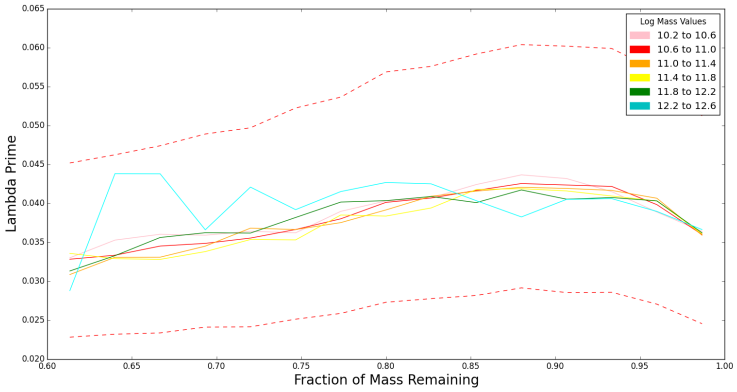

Figure 8. Lambda Prime vs Mass Remaining. The colored lines each represent the median value of lambda prime for halos in different mass ranges. The dotted lines shown above represent the dispersion of the data at its correspondingly-colored mass range at the 25th and 75th percentile levels for this figure as well all those that follow. Larger mass bins were removed due to small numbers of halos and excessive noise and distraction in the plot.

Figure 8 shows that the lambda prime values of halos with masses ranging from $10^{10.2} M_{\odot}$ to $10^{12.6} M_{\odot}$ generally converge at approximately 0.032 and 0.035 at the 40% and 0% levels of stripping, respectively. However, at around 0.90 mass remaining, all of the lines seem to reach a peak with a lambda prime value of around 0.040. There does not appear to be any relation of this particular occurrence to mass as the lines on the plot often overlap each other on the plot.

3.3 Prolateness and Axis Ratios

In our analysis of the prolateness, or level of elongation, and the axes ratios of halos, we gain valuable information on the shape of a halo.

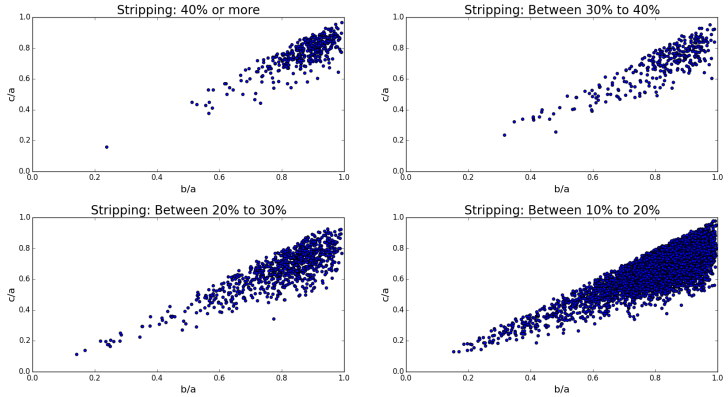

Figure 9. Axes Ratios of Halos. The figure above shows the axis ratios of halos with masses that range from $10^{11.0} M_{\odot}$ to $10^{11.4} M_{\odot}$ at four different levels of stripping. The lower left corners of the plots become significantly depopulated with a higher level of stripping.

As seen in Figure 9, extremely stripped halos tend to fall in the more spherical section of the graphs. However, there are still large numbers of halos at all degrees of elongation. Additionally, the lower right corners are significantly depopulated, signifying that although circular disk-shaped halos exist in theory, simulated halos do not follow such expectations.

Because we cannot easily tell by inspection how level of stripping affects the prolateness of a halo due to the sheer number of data points and the thick overlap, we must perform a two-sided K-S test as mentioned previously. The four graphs shown above were compared to the distribution of axes ratios of halos with a level of stripping between 0 to 10 percent. Performing a K-S test returned p-values that were larger than alpha, the significance level of 0.01 for the two bottom plots and p-values smaller than alpha for the top two. Therefore, we can conclude that, with a 0.01 level of significance, halos with less than a fraction of 0.7 mass remaining tend to be more spherical than halos with 0.9 or more mass remaining. As for halos with 0.1 to 0.3 mass remaining, we are not able to reject the null hypothesis that these halos do in fact have different shapes from those with more than 0.9 mass remaining.

3.4 Concentration

A graph of NFW concentrations can be seen below:

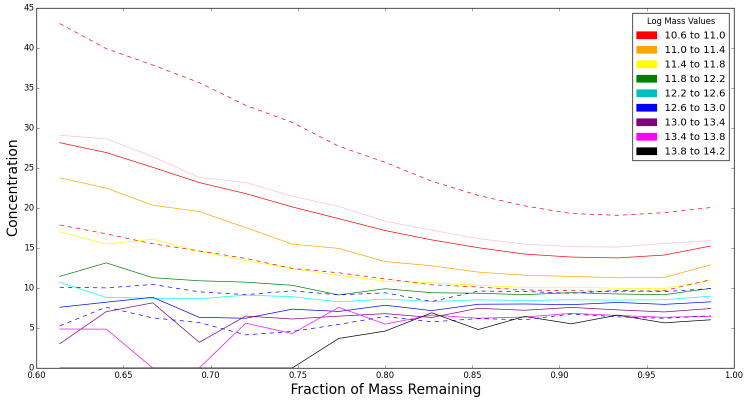

Figure 10. Concentration vs Mass Remaining. The figure above shows the median NFW concentration values for halos within different mass ranges, as represented by the differently colored lines. Like Figure 8, the dashed lines show a dispersion of the data at the 25th and 75th percentile levels.

The concentrations in the figure above show that concentration tends to increase with level of stripping, especially for halos with masses less than $10^{11.8} M_{\odot}$. Additionally, concentration sys-

tematically increases with a smaller mass range, as seen in the minimal overlap between the plots of the halos in different mass bins and consistently higher lines. The dispersion of the data is much larger for halos with a smaller mass than those with a larger mass.

Much like how in Figure 8, lambda prime reached a peak at 0.90 mass remaining, the inverse can be seen to be true in Figure 10. Concentration seems to reach a minimum at around 0.90 mass remaining, a curious discovery that has not yet been explored.

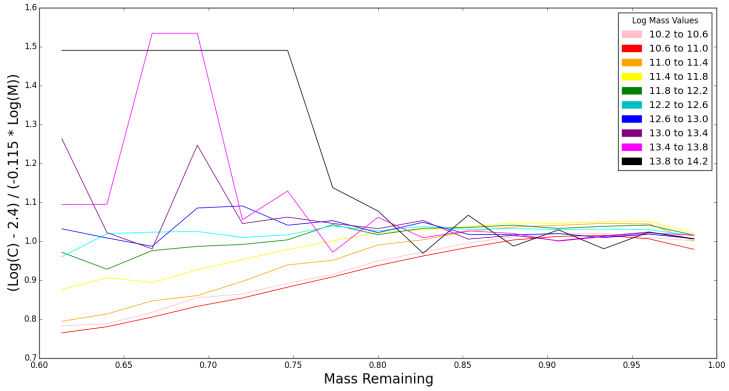

Figure 11. Scaled Concentration vs Mass Remaining. The figure above shows the scaled NFW concentration for halos at different mass ranges. The lines were scaled by finding the best fitting curve to the plot of $\log(M)$ vs $\log(c)$, where M is the mass and c is the NFW concentration.

In Figure 11, we can see that the green and blue lines are relatively straight, signifying that the concentrations of halos with masses that range from $10^{11.8}M_\odot$ to $10^{13.0}M_\odot$ have little correlation with the level of stripping. However, for halos outside of that mass range, we notice that concentration generally tends to increase with a larger mass, the opposite of what we observed with the unscaled concentration seen in Figure 10.

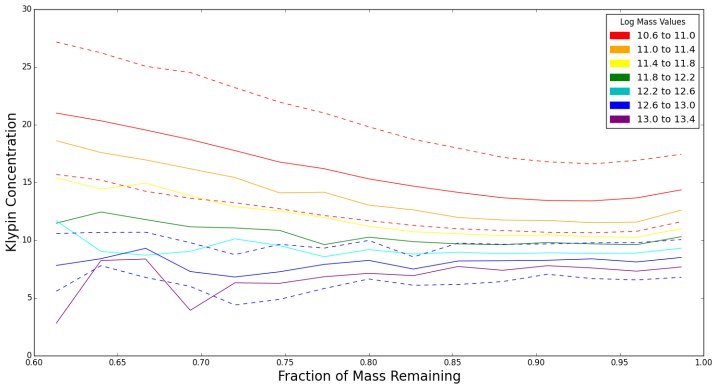

Figure 12. Klypin Concentration Levels. The figure above depicts the median values of the Klypin concentrations of halos with masses from $10^{10.6}M_\odot$ to $10^{14.2}M_\odot$ binned in sections of $10^{0.4}M_\odot$.

The Klypin concentrations of halos, derived by Anatoly Klypin, rely on finding the maximum circular velocity of the particles to determine the scale radius value (Klypin et al. 2011). Thus, unlike how the NFW concentration is calculated, the outer particles on a halo are not considered in the calculations for the Klypin concentration. As a result, the Klypin concentrations of halos with highly abnormal (e.g. extremely elongated) shapes tend not to be as artificially high. Such trends can be seen in Figures 10 and 12, where the NFW concentration values tend to be higher than the Klypin values.

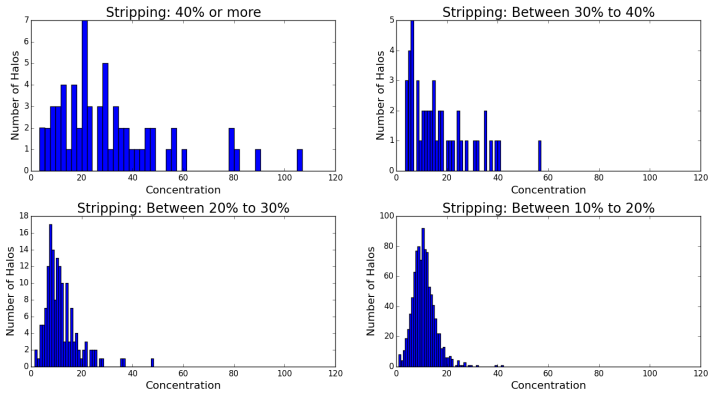

Figure 13. Concentrations of Halos. The four histograms above depict halo NFW concentrations at four different levels of stripping.

Concentration also seems to have a clear correlation to the level of stripping. From Figure 13, we see that a higher level of stripping usually relates to higher concentrations. Additionally, with higher levels of stripping, the histograms become more skewed to the right, signifying more halos with extremely high and abnormal concentration values.

4. Discussion

4.1 Implications of a 3-Parameter Fit

The densities of stripped dark matter halos generally fall off at a faster rate than their unstripped counterparts. When using the free exponent profile to model density profiles, the returned second-term exponent values are greater than 2, the value to which the NFW algorithm fits. Connecting this conclusion with our discovery of a characteristic bump in more stripped halos, it seems that whatever object is causing the dark matter halo to lose particles is in fact drawing them away. In

moving mass outwards, it creates that bulge, and as it begins to strip a larger percentage of mass, it affects a larger radius of the halo–thus, the steeper slope outside r_s.

4.2 Significance of Properties of Stripped Dark Matter Halos

From our results, we noticed that stripped halos tend to become more spherical with an increase in level of stripping. However, this pattern is a clear contrast from what we observed in the Bolshoi Planck simulation, where stripped halos were elongated on one or more sides of their centers. Studying the reasons for these differences as well as determining relationships between prolateness, lambda prime, and concentration to level of stripping can help us better understand dark matter halos, and by extension, dark matter.

4.3 Comparisons to Previous Research

Due to the very limited literature on stripped dark matter halos, we have not been able to verify or compare our results directly. However, as we have determined that the non negligible percentage of stripped halos and their distinct differences cannot be overlooked, their significance warrants more consideration in large scale simulations and algorithms that make calculations based off of the characteristics of normal, nonstripped halos only.

5. Conclusion

This study was one of the first to examine the properties of stripped dark matter halos relative to their percentage of mass lost and nonstripped halos. The results gained can be used for future classifications of dark matter halos and large scale simulations of our universe.

Lambda prime tended to decrease with a larger level of stripping. Additionally, the shapes of halos tended to become more spherical with more mass lost. The concentrations of stripped halos increases with level of stripping, a predictable result as it is likely that the loosely packed, lower-concentration outer particles are more likely to become stripped off compared to the more densely packed particles near the center of the halo. Additionally, we find that the NFW fit gives artificially low r_s values, which causes concentration to increase further.

We classify future work in our research into two areas: improving the quality of our data and furthering the study of the evolution and environment of stripped dark matter halos. Since we

only had access to a small portion of Bolshoi-Planck data, we will increase the number of halos of larger masses in particular to provide a more accurate view of relationships based on mass. In order to so, we will utilize the entirety of Bolshoi-Planck and look at data from other simulations like MultiDark that include a 1 Gpc/h box compared to Bolshois 250 Mpc/h box size (Klypin et al. 2011, 2014). Additionally, we will write an algorithm that filters out halos with multiple centers from those that have a single, distinct center so that the former type does not corrupt the characteristics that we are trying to determine about the latter.

Currently, all of our observations stem from the properties of stripped dark matter halos viewed at redshift zero. By examining the evolution of a halo over its lifetime, we will be able to see what role a halos environment might have on its likelihood of becoming stripped as well as follow merger trees to pinpoint which halos it interacted with to become stripped. We will explore these interactions further and classify them as either mergers or through-passes to see if specific types of collisions are more common or have different effects on the resulting characteristics of the stripped halos. Furthermore, by studying the history of a halo, we will determine why there is a local maximum value of lambda prime and a local minimum value of concentration at around a 0.90 fraction of mass remaining. Some current theories include looking at whether or not particles at the centers of halos behave differently from those that are slightly farther away.

As for the shape of stripped halos, we will investigate why our graphs seem to show that highly stripped halos appear more spherical while observing them by eye directly through the Bolshoi-Planck simulation predicts a more elongated shape. Some possible explanations include noting how the axis ratios are calculated in the tables. Because Rockstar uses the original spherical radius as the longest axis, we will see if other methods of determining axis ratios can explain the discrepancy.

Finally, although the 3-parameter fit seemed to follow the data more than the NFW fit did, based off of the smaller comparative error, we will also continue to try out different fitting functions to model the density distributions of stripped dark matter halos. We now know based off of the results of our 3-parameter fit that stripped halos tend to have a steeper drop off after r_s. In order

to model these steeper slopes, we will try adding another term to the denominator of the existing NFW function that will cause a third increase in magnitude of the slope as well as try different expressions altogether. Moreover, we hope to also determine a function that can account for the distribution past the bump and up until the r_{vir} value. From there, we will analyze the curvatures of these bumps and see if there are correlations to level of stripping.

Ultimately, as research into stripped halos is still only in its first stages, continued study into this field is encouraged. Since stripped halos make up a significant portion of all dark matter halos, learning more about their unique characteristics and causes as well as determining theoretical expressions that can accurately model stripped halo behavior is necessary before we can fully understand dark matter, and the universe at large.

References

[1] Allgood, B., Flores, R., Primack, J., et al. 2006, MNRAS, 1781, 1784, 1794

[2] Behroozi, P., Wechsler, R., Wu, H. 2013, AJ, 1, 3, 5

[3] Blumenthal, G., Faber, S., Primack, J., & Rees, M. 1984, Nature, 517

[4] Bullock, J., Dekel, A., Kolatt, T., et al. 2001a, AJ, 242

[5] Bullock, J., Kolatt, T., Sigad, Y., et al. 2001b, MNRAS, 564, 566

[6] Correa, C., Wyithe, J., Schaye, J., & Duffy, A. 2015, MNRAS, 1514

[7] Klypin, A., Kravtsov, A., Bullock, J., & Primack, J. 2001, AJ, 903, 908

[8] Klypin, A., Trujillo-Gomez, S., & Primack, J. 2011, AJ, 1

[9] Klypin, A., Yepes, G., Gottlber, S., Prada, F., & He, S. 2014, MNRAS, 1

[10] Navarro, J., Frenk, C., & White, S. 1996, AJ, 564, 567, 574

[11] Navarro, J., Frenk, C., & White, S. 1997, ApJ, 462, 563

[12] Navarro, J., Hayashi, E., Power, C., et al. 2004, MNRAS, 1039, 1043

[13] Prada, F., Klypin, A., Cuesta, A., et al. 2012, MNRAS, 3018, 3021, 3025

[14] Ramachandra, N. & Shandarin, S. 2015, MNRAS, 1643

[15] Schramm, D. 1993, AA, 13

[16] Vitvitska, M., Klypin, A., Kravtsov, A., et al. 2002, AJ, 799

[17] Zeeuw, T. & Franx, M. 1991, ARA&A, 244

[18] Zwicky, F. 1933, Helv. Phys. Acta, 6, 110